

P. Anjana<sup>1\*</sup>,  
A. Kumar<sup>1</sup>,  
N. Gupta<sup>2</sup>,  
V. Gupta<sup>2</sup>,  
H. P. Tiwari<sup>2</sup>

J. Electrical Systems 13-1 (2017): 131-142

Regular paper

**Optimization Based Shunt APF Controller  
to Mitigate Reactive Power, Burden of  
Neutral Conductor, Current Harmonics  
and Improve  $\cos\phi$**



This paper presents a Modified Gravitational Search Algorithm (MGSA) to improve the performance of PI controller in varying load condition. The proposed approach is capable of mitigating reactive power, neutral current, source current THD and significant improvement in power factor nearly unity (0.997). The DC link voltage across the capacitor is controlled by PI controller which is deciding the performance of shunt APF. Hence, the robust optimization technique based integral time square error (ITSE) with consideration of weight factor ( $\alpha$  &  $\beta$ ), maximum overshoot ( $|\Delta v_e(n)_{\max}|$ ) and settling time ( $t_s - t_0$ ), is providing the optimum solution of  $K_p$  &  $K_i$ . The robustness of proposed objective function and algorithm compared with GSA based three other error criterion techniques. The efficiency of the proposed controller has been tested over nonlinear and unbalance loading condition. The performance of ITSE based MGSA-PI controller is better than other three error criterion techniques. The values of THD are below the mark of 5% specified in IEEE-519 standard.

**Keywords:** Modified Gravitational Search Algorithm (MGSA), Integral Time Squared Error (ITSE), Shunt APF, Unity Power Factor (UPF), Total Harmonic Distortion (THD).

Article history: Received 1 June 2016, Accepted 11 January 2017

## 1. INTRODUCTION

From the past fifty years, the power quality pollution problem had been observed and tried to overcome the problem with the implementation of different techniques day-by-day [1]. At present every consumer is aware of power consumption and loss of power due to polluting loads. The power electronics based equipment are largely used in the present distribution system and these equipment are largely used semiconductor switches in the circuit; hence these switching losses create a problem in electric utility and deviate sinusoidal waveform. This deviation in sine wave is called as distortion and equipment are known as a non-linear load which leads to harmonic distortion. The non-linear loads are adjustable speed drives, arc furnaces, air conditioners, battery chargers, copier machines, computers, frequency converters, medical equipment, switch-mode power supplies, printers, uninterrupted power supplies, welding machines and x-ray equipment [2]. These harmonic currents degraded the quality of power and interact adversely with a wide range of power system equipment causing additional losses, overheating, overloading, interference with telecommunication networks and also results in erroneous readings in watt-hour and demand meters [3].

\* Corresponding author: Pradeep Anjana, Research Scholar Department of Electrical Engineering, MNIT Jaipur, India, E-mail: 2012ree9036@mnit.ac.in

<sup>1</sup> Research Scholar, Department of Electrical Engineering, MNIT Jaipur, India

<sup>2</sup> Faculty of Electrical Engineering, Department of Electrical Engineering, MNIT Jaipur, India

The evolution of different compensation techniques to remove the effect of the semiconductor switches from utility have been allowing a broader classification of the passive, active and hybrid power filter in power systems [4]-[7]. The merits and demerits of these methods are well presented in the literature [8]. One of the cornerstones of the shunt APF is its control scheme strategy. The popular reference current generation strategies are as unit template technique (UVT), power balance theory,  $I \cos\phi$  algorithm, current synchronous detection, PQ theory, SRF theory etc. One of the techniques is the DC link voltage control by closed-loop PI controller with UVT which is quite simple and practically used because of less number of sensors and switches used. The reference signal of the closed-loop feedback control method could be constant DC voltage which compares with DC link voltage of the capacitor. The useful information carried by the PI output signal is its wave shape rather than the place where it comes from.

The PI controller tuning is based on subspace estimation methods and prediction error estimation methods but they have some merits and demerits [8]. The subspace estimation methods are discussed as Process Reaction Curve method firstly proposed by Ziegler and Nichols for open loop and closed loop system [9], Relay method proposed by Astrm and Hagglund in 1995 [10], Tyreus-Luyben's method is proposed in 1997, Hagglund and Astrm's Robust tuning method, Skogestad's Model-based method and Setpoint Overshoot method etc [11]-[13]. Although these methods are widely used for tuning problems, but the manual estimation of PI parameters makes false tuning of PI. Others are prediction error estimation methods which are more popular in a present scenario. These methods are based on optimization problem. In that optimization series following methods are available Genetic Algorithm (GA) based PI, Particle Swarm Optimization (PSO) based PI, act colony optimization (ACO) based PI and fuzzy logic based PI and bacteria foraging optimization (BFO) based PI tuning etc [14]-[17]. The PSO is also an evolutionary computation technique that simulates the social behavior of a swarm of birds or school of fish. The main aspect of this technique is that the size and nonlinearity of the problem do not largely affect the solution.

In this paper, a modified GSA-PI is executed for gain scheduling of PI controller to minimize the error between the original DC link signal and the signal reference from the estimated parameters during the estimation process. The MGSA is presented for real-time self-tuning parameters, with Integral Time Square Error (ITSE) as an objective function. The model is simulated to show the performance of the proposed controller whether the sudden load change in micro grid under load change condition with the aim to study dynamic performance of the system.

This paper is organized as follows: In section II, proposed shunt APF principle, while section III describes the MGSA-PI controller. In section IV, the results and analysis with a component of the system under steady state condition are illustrated. Finally, conclusions out of the results will be shown in section V.

## 2. PROPOSED SAPF SCHEME AND ITS PRINCIPLE

The proposed topology of the SAPF is consists of a three-phase four wire based current controlled voltage-source inverter, a second-order low-pass filter with voltage feedback

loop as shown in Figure 1. Domestic consumers are using a large number of single-phase loads which are connected with one of the three-phases with neutral wire, so excessive neutral current will flow and cause reactive power burden and unbalance in the system. To overcome these problems four-wire active filters are developed [6]-[7]. They are classified as capacitor midpoint four-wire, four pole four-wire and three-bridge four-wire shunt active filter. Figure 1 shows four-pole switch type SAPF consists of four-leg VSI; three-legs are required to compensate the three-phase currents and one-leg needed to compensate the neutral current. The four-leg VSI consists eight IGBT switches and an energy storage capacitor. The indirect process is comparing with the modified controller and concludes the better feasible solution with practical implementation. The shunt-connected APF shows the characteristics similar to STATCOM (reactive power compensator of power transmission system) when used with self-controlled dc bus.

The schematic diagram of SAPF shown in Figure 1, mitigates harmonics from the current waveform by injecting equal and opposite current component. SAPF operated as current source injects harmonics generated by load but in phase opposition (i.e 180° phase shift). As a consequence the current harmonics in the load are canceling out by SAPF. This principle is considered for all type of non-linear loads. Harmonic distortion is seen in both types of waveforms due to electronic and non-linear loads. But it is evident that voltage harmonics are produced due to current harmonics only, so we have to mitigate only current harmonics from the supply to remove harmonic pollution from the system. That's why estimation of reference current is required [18].

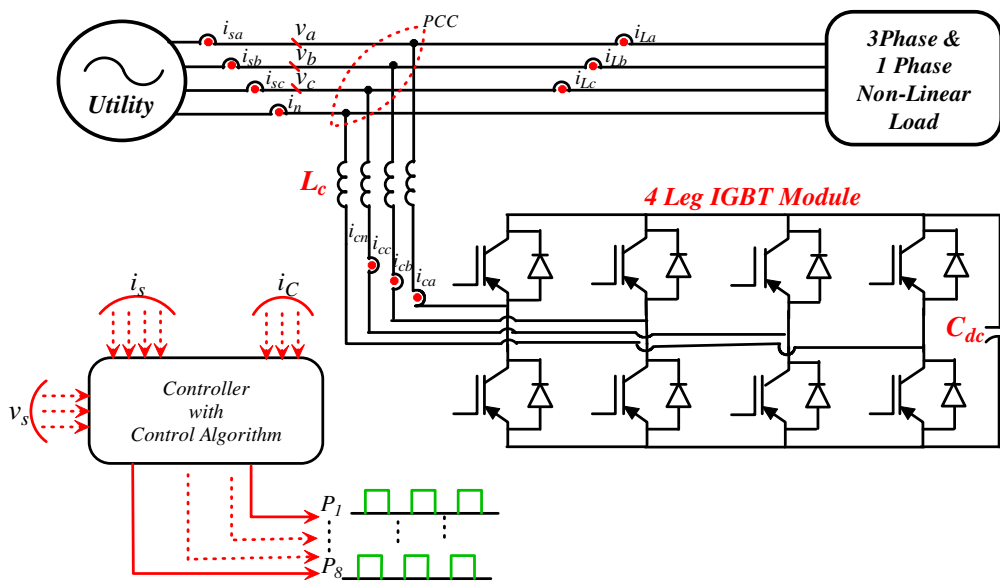


Figure 1. Proposed model of SAPF

For these purposes most applications requiring dynamic performance, pulse width modulation is the most commonly used for APF. Here hysteresis current controller technique applied to control the VSI for consists of chopping the dc bus voltage to produce an AC voltage of an arbitrary waveform. Gyugyi and Strycula [19] first introduced the concept of shunt active power filter. The controllers of shunt active power filters determines the compensating reference current in real time and force a power converter to

synthesize it correctly so that the filtering can be choosy and adaptive. Harmonic currents are produced mainly because of nonlinear loads and harmonic voltages in power system.

Figure 2 summarizes the basic principle of SAPF. A non-linear load draws a fundamental current component ( $I_{Lf}$ ) and load harmonic current component ( $I_{Lh}$ ) from the utility. Harmonic currents  $I_{Lh}$  flows through the power system, it produces a utility harmonic voltage drop ( $V_{Sh}$ ) equal to  $X_L \cdot I_{Lh}$ , that degenerates the load terminal voltage ( $V_T$ ). However, SAPF with shunt current compensation also draws an additional harmonic current ( $I_{Sh}$ ) from the utility. So this  $I_{Sh}$  further create a voltage drop ( $X_L \cdot I_{Sh}$ ) to keep the  $V_T$  sinusoidal and equal to  $V_{Sf} - X_L \cdot I_{Lf}$ , hence, the capacitor is charging/discharging and in this condition, the harmonic voltage components cancel each other, so that  $V_T$  is kept sinusoidal.

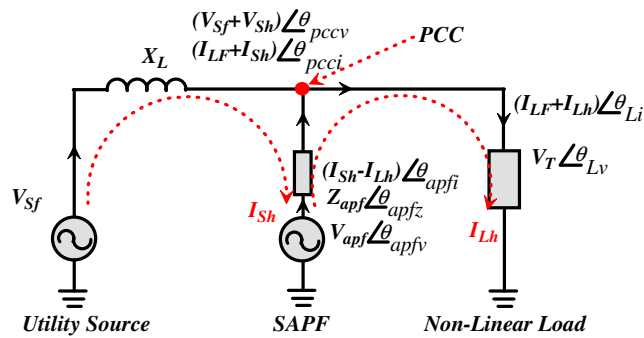


Figure 2. Principle of Shunt Current Compensation

An SAPF can compensate both harmonic currents ( $I_{Sh}$  &  $I_{Lh}$ ) when system impedance is high. However, the principle function of an SAPF is to restrict the load harmonic current at PCC, hindering its infiltration into the power system. In order to achieve these objectives, a Unit Vector Template (UVT) based indirect power control method, indirect PQ method is proposed with and MGSA-PI controller. The three main parameters:  $L_C$ ,  $V_{dc,ref}$  and  $C_{dc}$  are referred from [20]-[21]. From Figure 2, the instantaneous source currents and source voltage can be written as

$$\left. \begin{aligned} i_s(t) &= (I_{Lf} + I_{Lh} + I_{Sh}) \sin \omega t \\ \text{and} \\ v_s(t) &= V_m \sin \omega t \end{aligned} \right\} \quad (1)$$

A study of the nonlinear load has shown that the utility phase current will have a fundamental component with the presence of harmonic components (in the case of nonlinear load) which can be represented as:

$$\begin{aligned}
 i_s(t) &= \sum_{n=1}^{\infty} I_n \sin(n\omega t + \varphi_n) \\
 &\quad \text{(or)} \\
 &= I_1 \sin(\omega t + \varphi_1) + \sum_{n=2}^{\infty} I_n \sin(n\omega t + \varphi_n) \\
 &\quad \text{(or)} \\
 &= I_1 \sin \omega t \cdot \cos \varphi_1 + I_1 \cos \omega t \cdot \sin \varphi_1 + \sum_{n=2}^{\infty} I_n \sin(n\omega t + \varphi_n)
 \end{aligned} \tag{2}$$

Where

$I_1$  &  $I_n$  is the peak value of the fundamental and nth harmonic component of load current

$\varphi_1$  &  $\varphi_n$  is the phase angle of the fundamental and harmonic component of load current

$I_{Af}(t) = I_1 \sin \omega t \cdot \cos \varphi_1 =$  Active instantaneous fundamental load current

$I_{Rf}(t) = I_1 \cos \omega t \cdot \sin \varphi_1 =$  Reactive instantaneous fundamental load current

$I_{Hf}(t) = \sum_{n=2}^{\infty} I_n \sin(n\omega t + \varphi_n) =$  Harmonic instantaneous load current

The load power can be calculated as

$$\begin{aligned}
 p_L(t) &= v_s(t) \times i_s(t) \\
 &\quad \text{(or)} \\
 &= V_m \sin \omega t \times \left[ I_1 \sin \omega t \cdot \cos \varphi_1 + I_1 \cos \omega t \cdot \sin \varphi_1 + \sum_{n=2}^{\infty} I_n \sin(n\omega t + \varphi_n) \right] \\
 &\quad \text{(or)} \\
 &= V_m I_1 \sin^2 \omega t \cdot \cos \varphi_1 + V_m I_1 \sin \omega t \cdot \sin \varphi_1 \cdot \cos \omega t \\
 &\quad + V_m \sin \omega t \sum_{n=2}^{\infty} I_n \sin(n\omega t + \varphi_n) \\
 &\quad \text{(or)} \\
 &= P_A(t) + P_R(t) + P_H(t)
 \end{aligned} \tag{3}$$

Where

$P_A(t) = V_m I_1 \sin^2 \omega t \cdot \cos \varphi_1 =$  Instantaneous active power drawn by the load

$P_R(t) = V_m I_1 \sin \omega t \sin \varphi_1 \cos \omega t =$  Instantaneous reactive power demand of the load

$P_H(t) = V_m \sin \omega t \sum_{n=2}^{\infty} I_n \sin(n\omega t + \varphi_n) =$  Instantaneous harmonic power of the load

In the system, the reactive power is circulated between the phases before compensation. The SAPF compensator provides reactive power compensation. The utility will be liable only for the real power flow between utility and load [22]. The real power and current supplied by the utility during the compensation can be expressed as:

$$\left. \begin{aligned} P_A(t) &= V_m I_1 \sin^2 \omega t \cdot \cos \varphi_1 = v_s(t) \cdot I_1 \cos \varphi_1 \cdot \sin \omega t \\ &\text{or} \\ I_1 \cos \varphi_1 &= \frac{P_A(t)}{v_s(t) \sin \omega t} = \frac{V_m I_1 \sin^2 \omega t \cdot \cos \varphi_1}{V_m \sin \omega t \cdot \sin \omega t} \end{aligned} \right\} \quad (4)$$

Therefore, the peak value of active fundamental component of utility current is represented as

$$I_p(t) = I_1 \cos \varphi_1 \quad (5)$$

In a practical scenario, the current controlled VSI is also consumed some power in the form of switching, conducting and system leakage losses, which has to be supplied by the utility. So total peak current supplied by utility after compensation is given as

$$i_{SP} = I_p + I_{s_{loss}} \quad (6)$$

Where,  $i_{SP}$ = peak current supplied by utility after compensation and  $I_{s_{loss}}$  = total loss current of the system supplied by the utility.

After compensation, the flow of the loss component of current is between the utility and the SAPF, rather than total harmonic and reactive power of the load is supplied by the SAPF. So there is no harmonic component in the utility current. This makes the utility current to be in phase with the utility voltage. Therefore, the total instantaneous utility current including losses after compensation will be:

$$i_s^*(t) = i_{SP} \sin \omega t \quad (7)$$

Therefore, the injected current of SAPF will be given as

$$i_c(t) = (I_{Lf} + I_{Lh} + I_{Sh}) \sin \omega t - i_s^*(t) \quad (8)$$

So it is necessary to analyze the fundamental component of utility current, to circulate the information in closed loop control algorithm. Therefore, Power balance concept of the inverter depends on DC voltage error. This error signal is passed through a first order low pass filter (for eliminating the ripples) and then controller.

### 3. PI CONTROLLER TO MAINTAIN DC OFFSET VOLTAGE

The output of PI controller has been considered as DC loss of inverter, which is used to reduce steady state error of the dc-component and oscillatory component of active power [21]. The DC loss of inverter is estimated by calculating the peak DC supply current ( $\overline{i_{dc}}$ ) through capacitor using Vdc(n)voltage across the capacitor:

$$\overline{i_{dc}} = c \frac{dv_{dc}(n)}{dt} \quad (9)$$

The difference between actual dc bus voltage ( $\overline{v_{dc}}(n)$ ) and reference dc value ( $\overline{v_{dc,ref}}$ ) of nth sampling instant is expressed as  $\overline{v_e}(n)$ :

$$\overline{\Delta v_e}(n) = \overline{v_{dc,ref}} - \overline{v_{dc}}(n) \quad (10)$$

In order to regulate difference between actual dc bus voltage ( $\overline{v_{dc}}(n)$ ) and reference dc value ( $\overline{v_{dc,ref}}$ ), the error  $\overline{\Delta v_e}(n)$  is passed through the PI-regulator.

$$\overline{i_{dcp}} = K_p \overline{\Delta v_e}(n) + K_I \int \overline{\Delta v_e}(n) dt \quad (11)$$

The output of controller regulator at  $n^{\text{th}}$  sampling instant is known as peak error reference values ( $\overline{I_{dcp}}$ ) and it is used to circulate the information of reactive power demand/supply between SAPF and load. Hence, it is multiplied with unit sine vector template  $U_a$ , which is generated by the utility synchronizing angle obtained from zero crossing detector (ZCD) method, is known as the instantaneous reference current  $i_r^*$ . The values of  $K_p$  and  $K_i$  are decided by suitably considering the overshoot and settling time in transient response for a step change in dc voltage reference. The gains obtained by conventional methods are performing poorly during random load variations. Also, the coefficients of the characteristic equation are changing during load change condition. Hence, the transient response of the system is highly affected, because of transient response depends on damping ratio and natural frequency. So it is necessary to control the damping ratio and natural frequency by optimizing PI parameter [23]. Therefore, the evolutionary algorithms are used to find the optimized gains of PI controller in varying load condition by applying an 18 % load increase and decreases after four cycles.

### 3.1. Objective Function

In this case, regarding the control objectives, minimization of error integrating functions are used to minimization DC link error. The four error criterion techniques are implemented and tested on modified objective function [14]. Those error criterion techniques are as: Integral Absolute Error (IAE), Integral Square Error (ISE), Integral Time Absolute Error (ITAE), and Integral Time Squared Error (ITSE) and represent in equation (12).

$$\left. \begin{aligned} J_1 = ISE &= \int_0^{\infty} |\overline{\Delta v_e}(n)|^2 dt \\ J_2 = IAE &= \int_0^{\infty} |\overline{\Delta v_e}(n)| dt \\ J_3 = ITSE &= \int_0^{\infty} t * |\overline{\Delta v_e}(n)|^2 dt \\ J_4 = ITAE &= \int_0^{\infty} t * |\overline{\Delta v_e}(n)| dt \end{aligned} \right\} \quad (12)$$

From the above error, the objective function defined with consideration of weight factor ( $\alpha$  &  $\beta$ ), maximum overshoot ( $|\overline{\Delta v_e}(n)_{max}|$ ) and settling time ( $t_s - t_0$ ) is use as given below:

$$F = J * \beta + (1 - \beta)(t_s - t_0) + \alpha |\overline{\Delta v_e}(n)_{max}| \quad (13)$$

Where, J is the error function output ( $J_1/J_2/J_3$  or  $J_4$ ). At the first instance, to determine the optimum values of controller gain, the following parameters are chosen for the application of MGSA: population size (NP), maximum iteration (T), gravitational constants ( $G_0$ ), weight factor ( $\alpha$  &  $\beta$ ) and total number of agents ( $K_0$ ).

### 3.2. Implementation of MGSA

GSA is most commonly used heuristic algorithms based on Newton's laws of gravity and motion. All these objects attract each other by the force of gravity and this force causes a global movement of all objects towards the objects with a heavier mass. Hence masses co-operate using a direct form of communication through gravitational force. The heavy masses which correspond to good solution move more slowly than lighter ones, this guarantees the exploitation step of the algorithm [16]. In GSA, each mass (agent) has four specifications: position, inertial mass, active gravitational mass, and passive gravitational mass. The position of the mass corresponds to a solution of the problem and its gravitational and inertia masses are determined using a fitness function. In other words, each mass presents a solution and the algorithm is navigated by properly adjusting the gravitational and inertia masses. By lapse of time, it is expected that masses be attracted by the heavier mass. This mass will present an optimum solution in the search space. The GSA could be considered as an isolated system of masses. It is like a small artificial world of masses obeying the Newtonian laws of gravitation and motion. The basic GSA algorithm well defines in reference.

### 3.2.1. Iterative Algorithm for Proposed MGSA

GSA is characterized as a simple concept which is easy to implement and computationally efficient. In order to improve exploration and exploitation capabilities, GSA has a flexible and balanced mechanism. More precise search is achieved by assuming a higher inertia mass which causes a slower motion of agents in the search space. Faster convergence is obtained by considering a higher gravitational mass which causes a higher attraction of agents. GSA is a memory-less algorithm but works powerfully like the other memory-based algorithms. Nature inspired population-based techniques have proved themselves to be effective solutions to optimization problems control parameters and objective function are involved in these optimization techniques and appropriate selection of these parameters is a key point for success. It has been reported that GSA tends to find the global optimum faster than other algorithms and has a higher convergence rate for unimodal high-dimensional functions.

The final PI controller parameters corresponding to the minimization of DC link error is obtained by proposed objective function using values along with the system performance in terms of settling time, minimum damping ratio. The obtained results of different parameters are presented in Table 1.

Table 1 Tuned Controller Parameters and Performance Index for each Objective Function.

Objective function	Controller parameter		Maximum overshoot (in %)
	$K_p$	$K_i$	
J1:ISE	0.70	1.5	4.95
J2:IAE	0.37	0.735	6.20
J3:ITSE	0.13	0.85	3.80
J4: ITAE	0.35	0.92	5.90

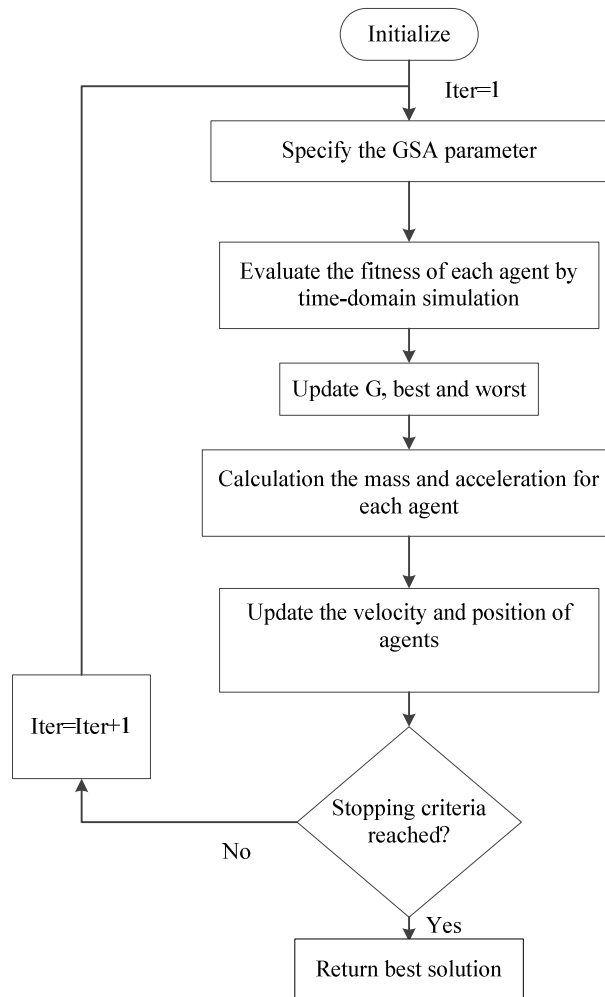


Figure 3. Flow chart of proposed MGSA optimization approach

To investigate the effect of objective function on the dynamic performance of the system, settling times (2% of final value) and peak overshoots in frequency and Vdc deviations along with minimum damping ratios are also provided. It can be seen from Table 1, that best system performance is obtained in terms of the maximum value of the damping ratio of system modes, minimum settling times, peak overshoots in frequency and Vdc deviations when ITSE is used as an objective function, minimum ITSE value is obtained with MGSA-PI.

#### 4. SIMULATION RESULTS

The robustness of proposed control algorithm is tested on MATLAB Simulink model. The results of shunt APF clearly shows the effectiveness of algorithm to mitigate reactive power, source current THD, neutral current and significant improvement in power factor in varying load condition. The initial values of optimization parameters and Simulink model are presented in appendix A.

The compensator is switched ON at  $t=0.05s$  and the integral time square error (ITSE) performance index is reported good performance of optimizing the PI coefficients. The balanced and sinusoidal three-phase source voltages are used for analysis purpose with highly nonlinear and unbalanced load characteristics profile. The THD in the load current is 27.05% before compensation but after compensation, it reduces to 3.52% approximately.

Figure 4 represent the source current and their THD performance with the different-different condition. The first oscillogram shows the source current and THD before compensation. Another oscillogram from 2nd to 5th represent the source current and their THD after compensation using IAE, ITAE, ISE and ITSE based objective function. The ITSE offered the best optimal values of PI controller to compensate power quality issue overall. In 5th oscillogram, the current in all phases are nearly balanced with a minimum flow of harmonic current in the system.

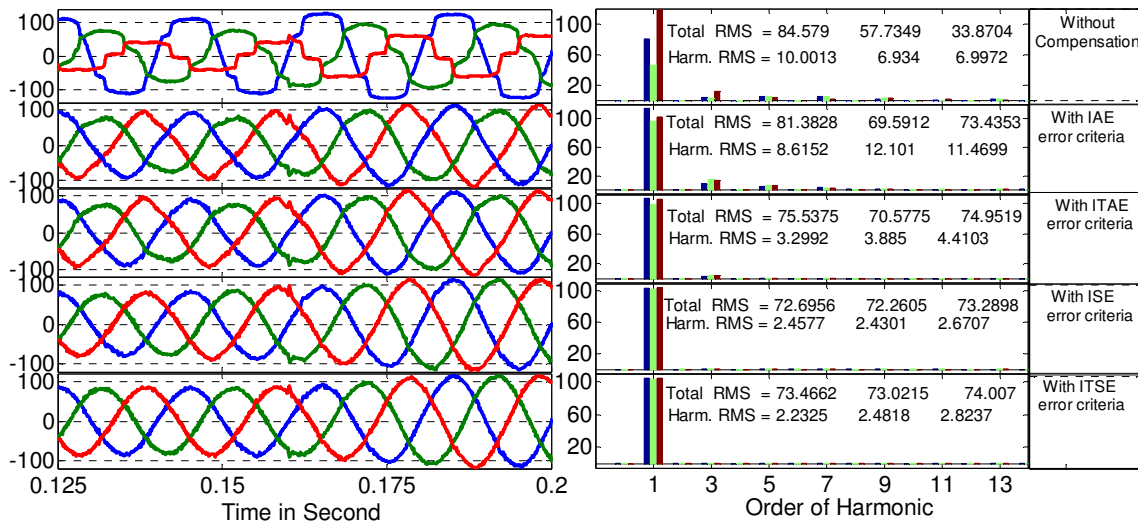


Figure 4. The source current with THD using MGSAoptimization based Shunt APF

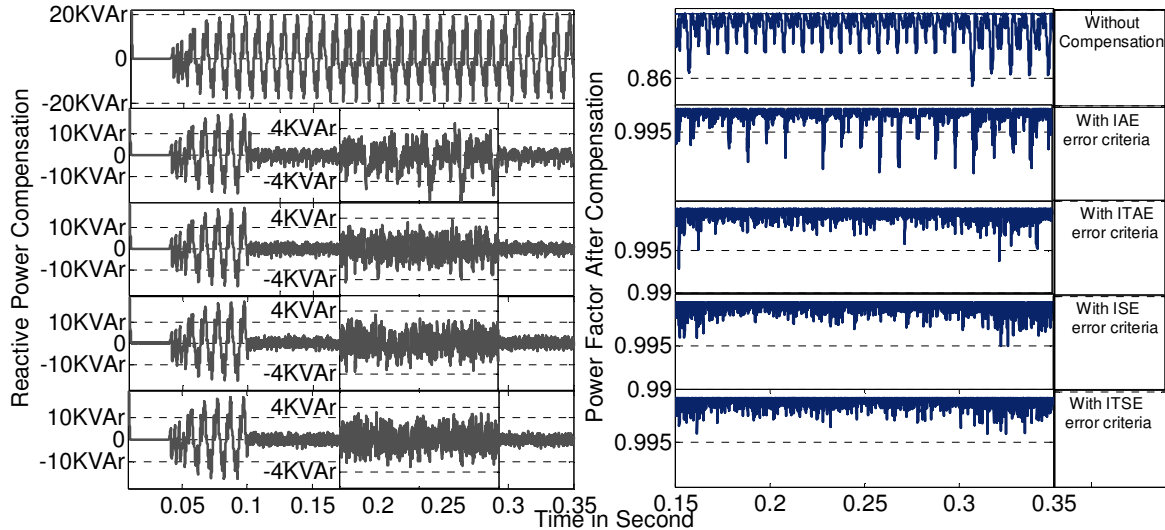


Figure 5. Reactive power compensation and Power factor improvement with MGSA optimization based shunt APF

Fig. 5 represent the reduction in the flow of reactive power between source and load. After compensation the reactive power consumed by nonlinear load flow between shunt APF and Load, hence, there is no effect seen in utility. Also, the power factor of utility is nearly 0.998 after compensation with ITSE based optimized shunt APF.

Figure 6 represents the neutral current compensation and counter harmonic current generated by the shunt APF with error optimized criteria techniques.

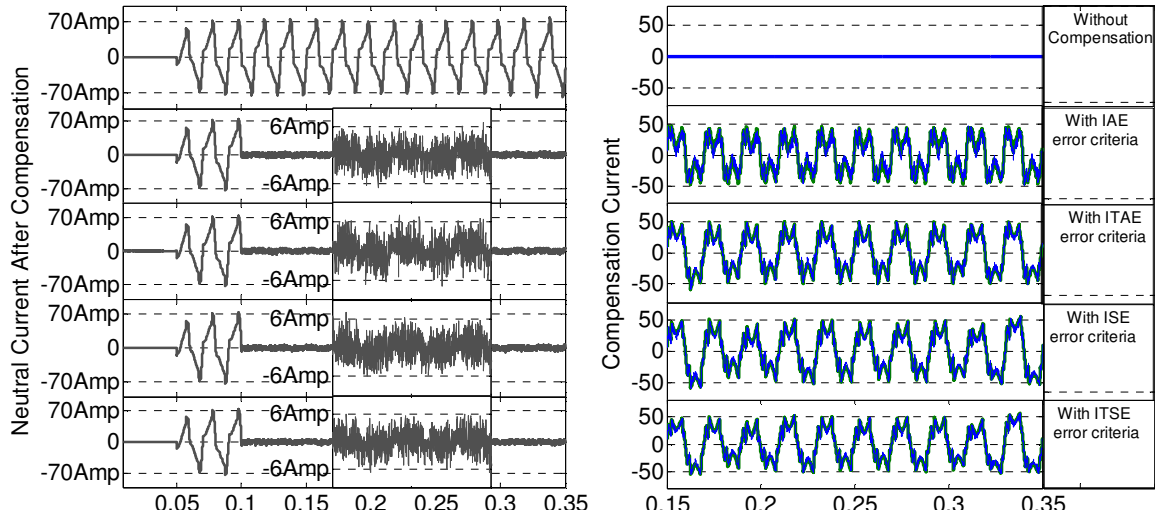


Figure 6. Neutral Current compensation and Compensating current with GSA based control strategy for Shunt APF.

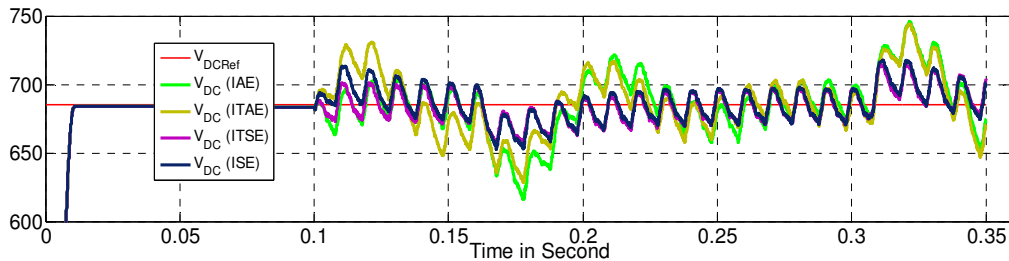


Figure 7. DC link voltage with variable load condition.

As represented in Figure 7, the stable point of DC link voltage decreases slightly due to a sudden connection/removal of the load. The ITSE objective function based PI controller performance is superior to compensates the load disturbance and the  $V_{dc}$  voltage remains equal to its reference  $V_{dc}$ . From the responses, it is depicted that the settling time required by the PI controller is approximately 8 cycles whereas in the case of ITSE optimized controller is about 6 cycles. The source current THD is reduced near to 4% in case of PI controller and 2.62% in case of ITSE optimized controller, which is below IEEE standard with both the controllers.

### 5. CONCLUSION

The optimization techniques are illustrated for tuning of PI controller in shunt APF. The objective function of optimization is tested with IAE, ITAE, ISE and ITSE based GSA optimization technique. Various simulation results are carried out to analyze the performance of the proposed technique. The performance of ITSE based GSA-PI controller is better than other error minimization technique. The heuristic modified GSA reported robust performance to control the power quality problem using shunt APF. The THD of the source current is below 5%, the harmonics limit imposed by IEEE standard.

### References:

- [1] IEEE Working Group on Power System Harmonics, "Power system harmonics: An overview," IEEE Transaction on Power Application Syst., vol. PAS-102, pp. 2455–2460, 1983.
- [2] J. S. Subjak and J. S. Mcquilkiln, "Harmonics-causes, effects, measurements, analysis: An update," IEEE Transactions on Industry Applications, vol. 26, pp. 1034–1042, 1990.

- [3] T. C. Shuter, H. T. Vollkommer and T.L. Kirkpatrick, "Survey of harmonic levels on the American electric power distribution system," IEEE Transaction On Power Delivery, vol. 4, no. 4, pp. 2204–2213, 1989.
- [4] H. Akagi, "Trends in active power line conditioners," IEEE Trans. Power Electronics, vol. 9, no. 3, pp. 263–268, 1994.
- [5] R.S. Herrera, P. Salmeron and H. Kim, "Instantaneous Reactive Power Theory Applied to Active Power Filter Compensation: Different Approaches, Assessment and Experimental Results," IEEE Transactions on Industrial Electronics, vol. 55, no. 1, pp. 184-196, 2008.
- [6] A. Kumar, H. Tiwari and P. Anjana, "Review of Active Power Filters for Improvement of Power Quality," INROADS- An international Journal of Jaipur National University, vol. 5, no. 1s, pp. 135-144, 2016.
- [7] S. Orts-Grau, F. J. Gimeno-Sales, A. Abellán-García, S. Seguí-Chilet and J. C. Alfonso-Gil, "Improved Shunt Active Power Compensator for IEEE Standard 1459 Compliance," IEEE Transactions on Power Delivery, vol. 25, no. 4, pp. 2692-2701, 2010.
- [8] R.S. Herrera and P Salmeron, "Instantaneous Reactive Power Theory: A Comparative Evaluation of Different Formulations," IEEE Transactions on Power Delivery, vol. 22, no. 1, pp. 595-604, 2007.
- [9] J. G. Ziegler and N. B. Nichols, "Optimum Settings for Automatic Controllers," Journal of Dynamic Systems, Measurement, and Control, vol. 115, no. 2B, pp. 220-22, 1993.
- [10] K. J. Astrom and T. Hagglund, "PID Controllers: Theory, design, and tuning, Research Triangle Park, N.C. International Society for Measurement and Control, 1995.
- [11] K.J. Astrom and T. Hagglund, "Automatic tuning of simple regulators with specifications on phase and amplitude margins," Automatica, vol 20, no. 5, pp. 645-651, 1984.
- [12] S. Skogestad and I. Postlethwaite, "Multivariable feedback control: analysis and design," vol. 2. New York: Wiley, 2007.
- [13] S. Dormido and F. Morilla, "Tuning of PID controllers based on sensitivity margin specification," in Proceedings of 5th Asian Control Conference, Melbourne, Australia, vol. 1, pp. 486-491, 2004.
- [14] R. K. Sahu , S. Panda and S. Padhan, "A novel hybrid gravitational search and pattern search algorithm for load frequency control of nonlinear power system," Applied Soft Computing, vol. 29, pp. 310-327, 2015.
- [15] U.K. Rout, R.K. Sahu and S. Panda, "Design and analysis of differential evolution algorithm based automatic generation control for interconnected power system," Ain Shams Engineering Journal, vol. 4, no. 3, pp. 409-421, 2013.
- [16] E. Rashedi, H. Nezamabadi-Pour and S. Saryazdi, "GSA: a gravitational search algorithm," Information Sciences, vol. 179, no. 13, pp. no. 2232-2248, 2009.
- [17] S. Panda, N.K. Yegireddy and S.K. Mahapatra, "Hybrid BFOA-PSO approach for coordinated design of PSS and SSSC-based controller considering time delays," International Journal of Electrical Power and Energy Systems, vol. 49, pp. 221–233, 2013.
- [18] L.B.G. Campanhol, S.A.O. da Silva and A. Goedel, "Application of shunt active power filter for harmonic reduction and reactive power compensation in three-phase four-wire systems." IET Power Electronics, vol. 7, no. 11, pp. 2825-2836, 2014.
- [19] L. Gyugi, and E.C. Strycula, "Active ac power filters", IEEE IAS Annual Meeting, pp. 529–53, 1976
- [20] W.H. Choi, C.S. Lam, M.C. Wong and Y.D. Han, "Analysis of DC-Link Voltage Controls in Three-Phase Four-Wire Hybrid Active Power Filters," IEEE Transactions on Power Electronics, vol. 28, no. 5, pp. 2180-2191, 2013.
- [21] S.B. Karanki, N. Geddada, M. K. Mishra and B.K. Kumar, "A DSTATCOM Topology With Reduced DC-Link Voltage Rating for Load Compensation With Nonstiff Source," IEEE Transactions on Power Electronics, vol. 27, no. 3, 2012.
- [22] R.M. Ciric, A.P. Feltrin and L.F. Ochoa, "Power Flow in Four-Wire Distribution Networks-General Approach," IEEE Transactions on Power Systems, vol. 18, no. 4, pp. 1283-1290, 2003.
- [23] P. Kumar and A. Mahajan, "Soft computing techniques for the control of an active power filter," IEEE Transactions on Power Delivery, vol. 24, no. 1, pp. 452-461, 2009.

*Appendix A*

Peak voltage and frequency V	328V,50 Hz
Supply /line inductance ,resistance	0.5mH,0.7 $\Omega$
Coupling inductance	3.5mH
For VS Type Load resistance	26.66 $\Omega$
For CS Type Load resistance, load inductance	26.66 $\Omega$ ,10 mH
For CS Single phase b/w c and n	36.66 $\Omega$ ,10mH
Single phase linear load b/w a and n	60 $\Omega$ ,10mH
Inverter DC( bus voltage and capacitance	685 V, 2200 $\mu$ F
population size NP	30
maximum iteration T	500
gravitational constants $G_0$	30
Weight Factor $\alpha = \beta$	10